



RESEARCH PAPER

Removal of Hg(II) Ions from Aqueous Environment with the Use of Modified LUS-1 as New Nanostructured Adsorbent

Farhang Azadegan¹ · Mehdi Esmaeili Bidhendi^{1,2} · Alireza Badiei^{3,4}

Received: 21 October 2018 / Revised: 9 April 2019 / Accepted: 30 April 2019 / Published online: 9 May 2019
© University of Tehran 2019

Abstract

A novel sorbent was developed for removal of mercury from water and characterized successfully. Response surface methodology was used for designing a model and optimization of the variable and hence, removal condition to obtain the maximum removal of mercury through batch process, i.e., minimum sorbent dose for maximum removal. The predicted optimum condition was validated experimentally. Three main factors including pH value of the solution, contact time, and sorbent dose were considered as variables of the models. Furthermore, combined effects of the factors were examined on the removal of the target species. The optimum values were obtained as 4.5, 25 min, and 55 mg L⁻¹ for pH value, contact time, and sorbent dose, respectively. All experiments were carried out on the basis of statistical designs to predict the predictive regression model. Maximum adsorption was obtained as 113.64 mg g⁻¹ through Langmuir model. Moreover, reusability and real sample test were performed and the results demonstrated high efficiency of the adsorbent in both experiments.

Article Highlights

- Recently, much attention has been focused on the fabrication of new easily regenerable, environmentally friendly, thermally/chemically stable and conveniently accessible materials for the removal of environmental pollutants, especially heavy metals. Nano structured porous adsorbents, due to their high specific surface area making them promising candidates for various applications such as chromatography, gas storage, sensors, catalysis, and adsorption.
- LUS-1 as part of Nano porous Silica materials can be easily functionalized or derivative on the desired choice especially in heavy metals adsorption processes. Thus, in this study, we reported the synthesis, characterization and adsorption behavior of novel modified LUS-1 for the adsorption of Hg²⁺ ions from aqueous environment and optimizing removal conditions with the use of response surface methodology (RSM).
- The synthesis of modified LUS-1 and successful exploration of its adsorption behavior towards Hg²⁺ ions has been reported for the first time. It is a new strategy for the adsorption of Mercury pollutants from aqueous media.

Keywords Hg(II) ions · Removal · LUS-1 · Nanostructure adsorbent · Aquatic environment

✉ Mehdi Esmaeili Bidhendi
Esmaeilib@ut.ac.ir

- ¹ Department of Environment, Kish International Campus, University of Tehran, Kish Island, Iran
- ² School of Environment, College of Engineering, University of Tehran, Tehran, Iran
- ³ School of Chemistry, College of Science, University of Tehran, Tehran, Iran
- ⁴ Nanobiomedicine Center of Excellence, Nanoscience and Nanotechnology Research Center, University of Tehran, Tehran, Iran

Introduction

The rapid expansion of various basic industries, have led to release of remarkable amounts of heavy metals to the environment, mainly through wastewater (Kadirvelu et al. 2001; Fu and Wang 2011). As heavy metals are not biodegradable, they can quickly accumulate in living organisms (Driscoll et al. 2013; Huang et al. 2015). Among these heavy metals, mercury is of significant concern due to its well-known highly toxic nature (Zhang et al. 2016). Widespread utilization of mercury in the vast variety of industries has exposed

living beings to copious pernicious effects (Di natale et al. 2006). It can severely damage the central nervous system and brain resulting in major motor disorders (Carvalho et al. 2008; Clarkson et al. 2003; Ding et al. 2015). Hence, the development of novel and efficient methods for the removal of mercury from water is highly demanded.

Porous materials have been a growing subject of extensive research due to their high specific surface area making them promising candidates for various applications such as chromatography (Nakanishi and Tanaka 2007), gas storage (Morris and Wheatley 2008), catalysis (Parlett et al. 2013), and adsorption (Raji and Pakizeh 2013; Bidhendi et al. 2014; Shahabuddin et al. 2018). Ordered nanoporous silica materials including SBA-15, MCM-41, and LUS-1 (Hamad et al. 2008), the structures of which consists of a combination of organic and inorganic blocks are particularly attractive because they provide the advantage of the introduction of flexible organic moieties onto the solid inorganic structure. Grafting and co-condensation approaches are the two widely used methods for incorporation of organic groups onto the surface of these materials (Hoffmann et al. 2006). Other than remarkably high specific surface area, ordered nanoporous silica materials are characterized by highly uniform pores where target species can readily diffuse to meet the grafted organic groups capable of adsorption of the species. Furthermore, thick walls, and biocompatibility of ordered porous materials, as well as their high thermal stability makes them significantly important candidates for adsorption purposes in different environmental conditions (Hartmann 2005). Despite precious characteristics including relatively narrower pore channels impeding diffusion of large species to the channels which in turn improves the selectivity of the adsorbent (Karimi et al. 2015), to the best of our knowledge, LUS-1 has not been used for adsorption of contaminants to date.

Adsorption as a versatile and simple water treatment technique is widely used in wastewater treatment. In this study, response surface methodology (RSM) as a highly efficient method utilizing mathematical equations to help understand the interaction between different parameters and design experiments to save time and costs (Sahu et al. 2009). To the best of our knowledge, no report has been published about using response surface methodology for investigation and optimization of adsorption of toxic species including Hg(II) by a sorbent based on LUS-1.

Experimental

Materials and Reagents

Nitric acid, hydrochloric acid, ethanol, toluene, sodium hydroxide, mercury nitrate dehydrates, Ludox HS-40 (40%

SiO₂), hexadecyltrimethylammonium-*p*-toluene-sulfonate (CTATos), bis-(triethoxysilylpropyl) sulfide, were all purchased from Sigma Aldrich Company.

Apparatus

A MIRA (TESCAN) scanning electron microscopy was used to take SEM images. A Philips X'Pert PW 3040/60 diffractometer with Cu-K_α radiation ($\lambda = 1.542 \text{ \AA}$) was used to record low angle X-ray diffraction patterns. FT-IR spectra were obtained within the range of 600–4000 cm⁻¹ on a RAYLEIGHT WQF-510A spectrometer using KBr disks. A BELSORP-mini II was utilized to acquire N₂ adsorption–desorption isotherms at liquid nitrogen temperature (– 196 °C). Brunauer–Emmett–Teller (BET), Barrett–Joyner–Halenda (BJH) equations and BELSORP analysis were used to estimate physical properties of the synthesized materials such as specific surface area, pore volume, pore diameter, and pore size distribution. Thermogravimetric analysis were performed on a TGA Q50 V6.3 Build 189 instrument with a ramp rate of 10 °C min⁻¹ from room temperature to 1000 °C in the air. An atomic adsorption with high resolution continuum source (Analytic Jena AG-contrAA 700, Germany) was used to record UV–Vis absorption spectra in between 200 and 1100 nm).

Synthesis of the Sorbent (LUS-1)

LUS-1 was prepared following a two-step procedure, LUS-1 was synthesized and characterized successfully, and then in the second step it was functionalized by bis-(triethoxysilylpropyl) disulfide to obtain the final product. Further details are provided in the supplementary information.

Synthesis of LUS-1: LUS-1 was synthesized according to a previously reported procedure in the literature (Badiei et al. 2006). 2 g sodium hydroxide was dissolved in 50 mL deionized water, to which solution 15.5 g Ludox was added. The mixture was stirred at 40 °C for 24 h. Another solution was then prepared by addition 2.5 g of hexadecyltrimethylammonium-*p*-toluenesulfonate (CTATos) to 90 mL deionized water and stirring at 60 °C for approximately 1 h. The first solution was then added slowly to the second solution and stirred at 60 °C for 2 more hours. The obtained mixture was transferred to a Teflon-lined autoclave and left to stand at 130 °C for further condensation (20 h). Finally, the synthesized product was filtered and washed with excess amount of water (1000 mL) and then dried at 80 °C (Abry et al. 2005).

Modified LUS-1: 1 g of the previously synthesized and dried LUS-1 was added portion wise to 100 mL dry toluene and stirred until a homogeneous suspension was obtained. 2 mmol of bis(triethoxysilylpropyl)disulfide was added slowly to the suspension and the mixture was refluxed for

6 h. The obtained product was filtered off, washed with toluene and then with ethanol, and finally dried at ambient temperature.

Adsorption experiments

Batch method was applied to investigate effects of three different parameters (pH, contact time, and sorbent dose) on removal of mercury from water and obtain the optimal condition. Hg(II) solutions (2.5 ppm) were prepared by dilution of a stock solution (1000 ppm), which was prepared by dissolution of Hg(NO₃)₂ in water. Concentration of Hg(II) ion in the media was determined before and after sorption process. pH of the solutions was adjusted using nitric acid. All batch experiments were performed at ambient temperature and a shaker with 500 rpm was used for stirring the solutions. Impact of several variables including pH value of the solution, contact time, and sorbent dose was studied through response surface methodology (RSM). This method as a collection of mathematical and statistical technique examines relationship between several parameters. Amount of the adsorbed ions per specific amount of sorbent is called adsorption capacity (*q*), which was obtained by the following equation (Esmaeeli et al. 2017):

$$q = (C_i - C_e) \times \frac{V}{m}, \tag{1}$$

where *q* represents amount of adsorbed Hg(II) on the sorbent (mg g⁻¹), *V* is volume of the solution (L), *C_i* represent initial concentration (mg L⁻¹), *C_e* is equilibrium concentrations of the metal-ion (mg L⁻¹), and *m* stand for the sorbent weight (g).

Once the initial and equilibrium concentrations of Hg(II) ion is known, it is possible to further calculate the removal efficiency (% *R*) of Hg(II) ions by the following equation:

$$(\%R) = \frac{C_0 - C_e}{C_0} \times 100\%. \tag{2}$$

Experimental Design

The objective of this work is to investigate the removal efficiency of Hg(II) ion from water using RSM. Design Expert software 7.1.3 was used to remove systematical errors and to estimate experimental errors and minimize the number of experiments as well (Antochshuk et al. 2003; Saleh et al. 2017). Central composite design (CCD) was used to assess the relationship between independent parameters and responses, and subsequently optimize the conditions accordingly CCD requires three levels as low, central, and high. These levels were coded for statistical analysis through Eq. 3 as - 1, 0, and + 1, respectively. Optimal values for selected parameters were obtained through regression equation. Pre-tests were carried out to determine the experimental range, which is provided in Table 1.

Overall, 15 experiments were generated to evaluate effects of the three variables on adsorption of mercury. The experiments were carried out by adjusting values of the three variables to certain numbers obtained from the software. Results of CCD experiments acquired by investigation of effects of the three parameters are presented in Table 2.

Independent parameters were coded by the following equation (Eq. 3) for later statistical studies.

$$x_i = \frac{X_i - X_0}{\Delta X_i} \tag{3}$$

where *x_i* stands for the coded value, *X_i* is the real value *X₀* is the real value at the center point and ΔX_i stands for step change value.

Mathematical Modeling

RSM optimization process, takes advantage of first and second-order models to obtain the desired results. The experiments determined that each parameter could only appear in three levels. Hence, the second-order model was selected as

Table 1 Experimentally obtained ranges and levels for the independent parameters

Design summary											
Study type		Response surface				Runs		15			
Initial design		Central composite				Blocks		No blocks			
Design model		Quadratic									
Factor	Name	Units	Type	Low actual	High actual	Low coded	High coded	Mean	Std.Dev		
A	pH		Numeric	3.00	6.00	- 1.00	1.00	4.50	1.23		
B	time		Numeric	10.00	25.00	- 1.00	1.00	17.50	6.12		
C	sorbent		Numeric	25.00	55.00	- 1.00	1.00	40.00	12.25		
Response	Name	Units	Obs	Analysis	Minimum	Maximum	Mean	Std.Dev	Ratio	Trans	Model
Y1	Removal		15	Polynomial	0.798	0.999	0.937	0.062	1.251	None	Rquadratic

Table 2 Matrix of the designed experiments

Run	Factor 1: pH	Factor 2: time (min)	Factor 3: sorbent (mg)
1	1.90	17.50	40.00
2	4.50	17.50	40.00
3	7.10	17.50	40.00
4	3.00	25.00	55.00
5	4.50	4.51	40.00
6	4.50	17.50	40.00
7	4.50	17.50	65.98
8	4.50	30.49	40.00
9	4.50	17.50	40.00
10	4.50	17.50	14.02
11	4.50	17.50	40.00
12	3.00	10.00	25.00
13	6.00	25.00	25.00
14	4.50	17.50	40.00
15	6.00	10.00	55.00

the appropriate model (Eq. 4) (Bhatti et al. 2017). This also includes the first-order model

$$Y = \beta_0 + \sum \beta_i X_i + \sum \beta_{ii} X_i^2 + \sum \beta_{ij} X_i X_j + \varepsilon \quad (4)$$

where Y stands for the predicted response, X_i, X_j, \dots, X_{ij} are the parameters, $X_i^2, X_j^2, \dots, X_k^2$ are the square effects, β_0 is the intercept, β_i ($i = 1, 2, \dots, k$) stand for regression coefficients for linear effects, β_{ii} ($i = 1, 2, \dots, k$) is regression coefficient for square effects, β_{ij} ($i = 1, 2, \dots, k; j = 1, 2, \dots, k$) is regression coefficient for interaction effect, ε presents a random error and k is the number of investigated parameters. Probability (P) values with a 95% confidence were used to either confirm or reject the model terms. The results were thoroughly analyzed by analysis of variance (ANOVA) (Sharifzadeh Baei et al. 2016).

Results and Discussion

Low Angle X-ray Diffraction

A low angle XRD pattern of the synthesized LUS-1 before and after modification is provided in Fig. 1. Three distinctive reflections were observed in both patterns with relatively lower intensities in the case of the modified LUS-1, which could be assigned to incorporation of organic groups into the pore walls of LUS-1 leading to partially lower long-range order. A sharp reflection at about $2\theta = 2^\circ$ as well as two other reflections at around $3.5^\circ < 2\theta < 4.5^\circ$

associate with hexagonal structure of the pore channels of ordered mesoporous materials. Appearance of all three reflections in the XRD pattern of the modified LUS-1 verifies preservation of the meso-structure (Hosseini et al. 2013; Gholami et al. 2009; Badieli et al. 2009) during the modification process (Fig. 1).

SEM Analysis

The morphology of the modified LUS-1 is analyzed using the scanning microscopy (SEM) for which its appearance is presented (Fig. 2) and the long rod-shaped characters by the size of 100 nm are apparent.

Nitrogen Adsorption–Desorption

Figure 3 illustrates physical properties of the synthesized modified LUS-1 through nitrogen adsorption–desorption analysis. N_2 adsorption–desorption analysis of adsorbent demonstrates a type IV isotherm with an H1-hysteresis loop corresponding to the cylindrical structure of the meso-structure (Shiravand et al. 2012). Also, the hysteresis loop in the isotherm indicates preservation of the structure of LUS-1 after incorporation of organic moieties onto the surface of LUS-1 (Karimi et al. 2015). The pore volume, the pore diameter, and the pore size distribution of modified LUS-1 are $0.7099 \text{ cm}^3 \text{ g}^{-1}$, $786.4946 \text{ m}^2 \text{ g}^{-1}$ and 3.6105 nm , respectively. These results depict the large surface of adsorbent is imprinted.

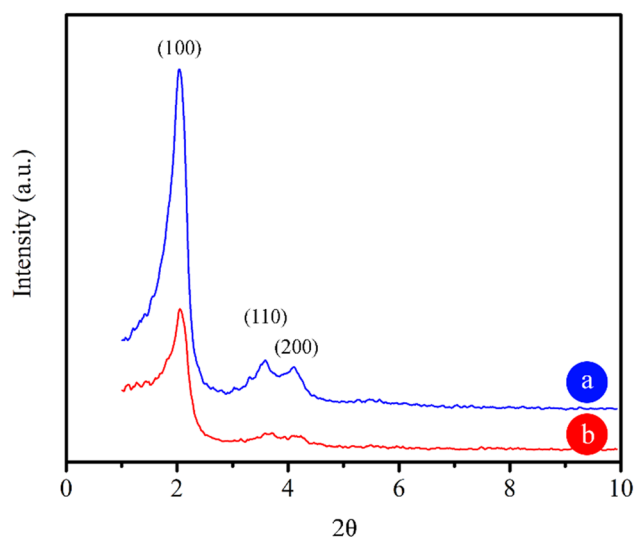


Fig. 1 Low angle powder XRD patterns of a. LUS-1 and b. Modified LUS-1

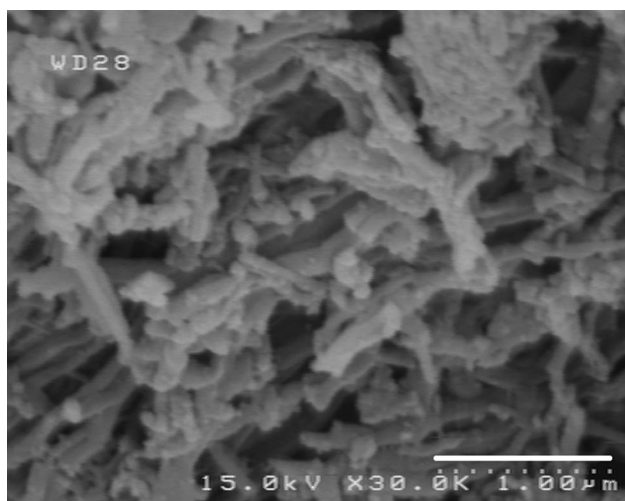


Fig. 2 SEM image of LUS-1

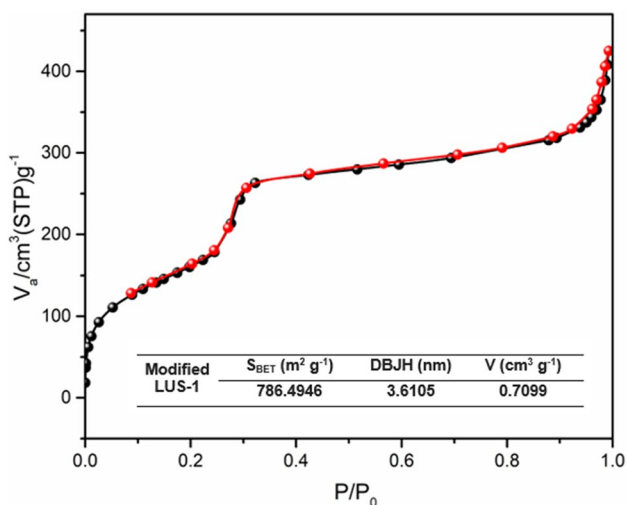


Fig. 3 N₂ adsorption–desorption isotherms of modified LUS-1

FT-IR Spectroscopy

FT-IR spectrum was recorded to confirm successful incorporation of organic groups into the pore channels of LUS-1. The strong bands observed at around 1100 cm^{-1} in the spectra of both materials are assigned to stretching vibrations of Si–O–Si structure. The band observed at about 1630 cm^{-1} can be assigned to vibrations of physically adsorbed water molecules onto the surface of the meso-structures. Two new bands emerged in the spectrum of modified LUS-1 (Fig. 4b) in between 2900 and 3000 cm^{-1} , which were not observed in the spectrum of LUS-1 (Fig. 4a). These bands are due to symmetric and asymmetric vibrations of C–H groups and confirm successful

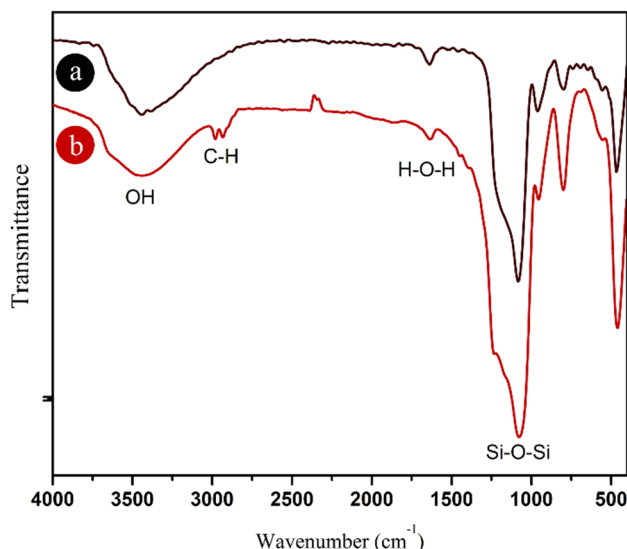


Fig. 4 FT-IR Spectra of a. LUS-1 and b modified LUS-1

introduction of bis(triethoxysilylpropyl)disulfide groups with C–H bonds on the propyl groups.

(TGA/DTA) Measurement

Thermogravimetry analysis was carried out to estimate the amount of organic groups incorporated into the pore channels of LUS-1. TGA curve for modified LUS-1 is provided in (Fig. 5), in which an initial weight loss is observed from room temperature up to as high as approximately 250 °C, which is normally considered to be due to removal of physically adsorbed water and probably other volatiles from the meso-structure. The subsequent major weight loss of about 13% starting from 250 °C was due to decomposition and removal of organic moieties grafted onto the

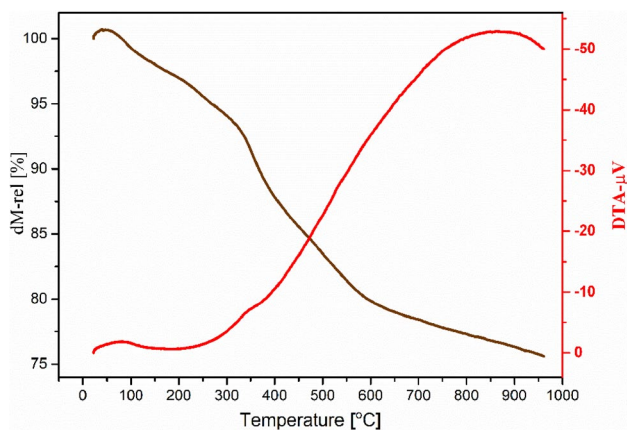


Fig. 5 TGA/DTA analysis of modified LUS-1

surface of LUS-1. This was used to estimate the amount of organic groups successfully attached to the surface of LUS-1 as 1.67 mmol g⁻¹.

Statistical Analysis

In many scientific phenomena, it is not normally possible to develop an appropriate model only based on mathematics due to the contribution of a wide variety of parameters. In these cases, one can develop an experimental-based model, in which method the experiments can be designed using certain software to save time and reduce the expenses. In current work, CCD as the most popular RSM design was used to develop the least but an inclusive number of experiments to obtain the optimum condition for removal of mercury ion from water (Saleh et al. 2017). Initial experiments demonstrated the influence of pH of the solution, contact time and sorbent dose in the removal of Hg(II) ion. CCD was used to study the interactions between these three different variables (pH, contact time, and sorbent dose in the range of 3–6, 10–25 min, and 25–55 mg L⁻¹, respectively) and their impact on removal of the Hg(II) ion. On the basis of these inputs, a matrix with 15 experiments was obtained from the software, the results of which for both predicted and actual values are presented in Table 3 as well as experimental and response values.

As a statistical technique, analysis-of-variance (ANOVA) was carried out to the hypothesis on the parameters of the model and justify the adequacy of the model. The results

obtained from ANOVA for significance and accuracy of the model are provided in Table 4. Based on (Eq. 1), significance and validity of the model is verified by *F* and Probe > *F* factors (Shahabuddin et al. 2018). According to the designed model *P*-values higher than 0.1 are not considered significant. However, those below 0.05 are significant, and therefore, effective on the output results. *F*-values may further emphasize the significance of certain parameters. Therefore, as can be seen in Table 4, the sources *A*, *B*, *C*, *AB*, and *A*² are recognized as the significant model terms. The *F*-value was obtained as 25.92, which implied that the model was significant. In addition, the low value of 0.23 for Lack of Fit further indicated that the second-order model was appropriate.

The suggested design is a quadratic polynomial model. The proximity of the predicted R-square and adjusted R-square values, which are provided in Table 5 indicate adequacy of the selected model. Furthermore, one can verify the efficiency of the model based on *R*² = 0.93 and Adec. Precision = 16.414.

The high value of the model coefficient of determination (*R*²) suggests the statistical significance of the regression. The high value of the model coefficient of determination (*R*²) suggests the statistical significance of the regression. (*R*²) value defines that an excellent model would be able to predict a response value sufficiently. According to Table 1, the numerical approximation of the *R*-value for predicted determination and adjusted determination depicts a good agreement. Finally, the

Table 3 Predict and actual values

Response	1	Removal	Transform		Internally	Externally	Influence on		
Standard	Actual	Predicted	Residual	Leverage	Studentized	Studentized	Fitted Value	Cook's	Run
Order	Value	Value			Residual	Residual	DFFITs	Distance	Order
1.00	0.92	0.92	- 3.95E-03	0.523913	- 0.28	- 0.27	- 0.28	0.01	13.00
2.00	0.99	0.99	- 4.72E-04	0.523913	- 0.03	- 0.03	- 0.03	0.00	15.00
3.00	0.98	0.98	1.28E-04	0.523913	0.01	0.01	0.01	0.00	4.00
4.00	0.82	0.81	3.60E-03	0.523913	0.26	0.24	0.25	0.01	12.00
5.00	0.80	0.80	- 2.24E-03	0.7217391	- 0.21	- 0.20	- 0.32	0.02	1.00
6.00	0.91	0.90	2.47E-03	0.7217391	0.23	0.22	0.35	0.02	3.00
7.00	0.91	0.92	- 8.55E-03	0.3956522	- 0.54	- 0.52	- 0.42	0.03	5.00
8.00	1.00	1.00	- 4.54E-03	0.3956522	- 0.29	- 0.27	- 0.22	0.01	8.00
9.00	0.90	0.91	- 1.36E-02	0.5956522	- 1.05	- 1.06	- 1.28	0.27	10.00
10.00	1.00	1.01	- 1.36E-02	0.5956522	- 1.05	- 1.06	- 1.28	0.27	7.00
11.00	0.99	0.96	3.26E-02	0.0956522	1.68	1.91	0.62	0.05	6.00
12.00	0.98	0.96	1.58E-02	0.0956522	0.81	0.80	0.26	0.01	14.00
13.00	0.92	0.96	- 3.82E-02	0.0956522	- 1.97	- 2.46	- 0.80	0.07	2.00
14.00	0.98	0.96	1.34E-02	0.0956522	0.69	0.67	0.22	0.01	9.00
15.00	0.98	0.96	1.71E-02	0.0956522	0.88	0.87	0.28	0.01	11.00

Table 4 ANOVA results for response surface model

Analysis of variance table (partial sum of squares–type III)						
	Sum of Squares	df	Mean Square	F Value	p value	Prob > F
Source						
Model	0.053983283	5	0.010796657	25.91537318	< 0.0001	Significant
A-pH	0.008770446	1	0.008770446	21.05183059	0.0013	
B-time	0.005469116	1	0.005469116	13.127599	0.0055	
C-sorbent	0.005073166	1	0.005073166	12.17719405	0.0068	
AB	0.002161915	1	0.002161915	5.189275127	0.0487	
A ²	0.020703452	1	0.020703452	49.69479945	< 0.0001	
Residual	0.003749508	9	0.000416612			
Lack of fit	0.000836934	5	0.000167387	0.229881481	0.9307	Not significant
Pure error	0.002912575	4	0.000728144			
Cor Total	0.057732792	14				

Table 5 Variance data analysis of response surface

Std. Dev.	0.020411077	R ²	0.935054095
Mean	0.937304162	Adj R ²	0.898973036
C.V. %	2.177636393	Pred R ²	0.882859676
PRESS	0.006762838	Adeq Precision	16.41441593

second-order polynomial equation was obtained as follows (Eq. 5):

$$\begin{aligned} \text{Removal (Hg(II))} = & 0.96 + 0.030 \times A + 0.023 \\ & \times B + 0.029 \times C - 0.030 \\ & \times A \times B - 0.037 \times A^2. \end{aligned} \tag{5}$$

The predicted results and actual experimentally obtained results for absorption of mercury are provided in Fig. 6. Actual and predicted values are obtained from measured response data for a particular run and from the model which were generated through proximity functions, respectively. The plot illustrates the relationship between the predicted and actual values. As observed, the majority of the responses demonstrate maximum removal values, and proximity of the values to the linear plot verifies that the model is appropriate.

Effect of Various Parameters on Adsorption of Mercury

Response surface methodology was used to study effects of three different factors including pH value of the solution, contact time, and sorbent dose on adsorption of mercury. Two and three dimensional diagrams are drawn for investigation of each factor.

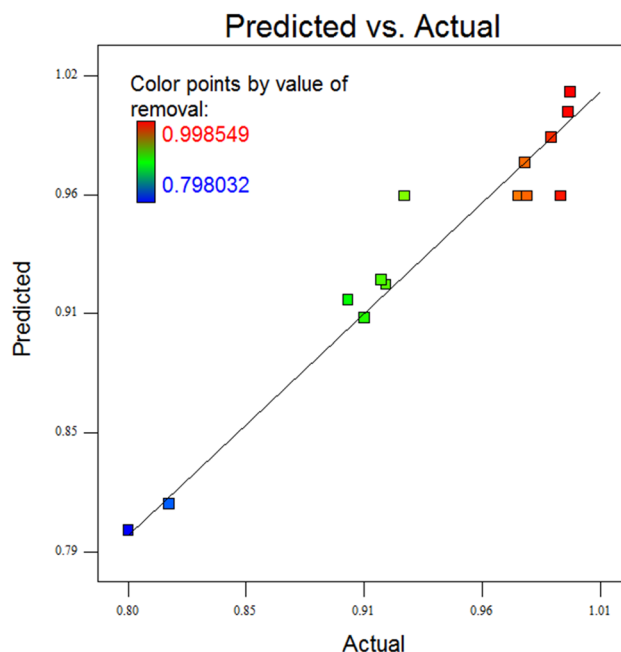


Fig. 6 Predicted and actual values for absorption of Hg(II) ions

Effect of pH

pH value of a solution plays a highly important role in wastewater treatments. Optimization of pH value of the solution can contribute remarkably to the removal of toxic species from wastewater and reduce the costs considerably. Therefore, the effect of different pH values was investigated on the removal of mercury in the range of 3–6. As demonstrated in Fig. 7, removal of mercury increased by increasing the pH value up to 4.5, where the maximum value was reached and then declined by further increase of the pH values.

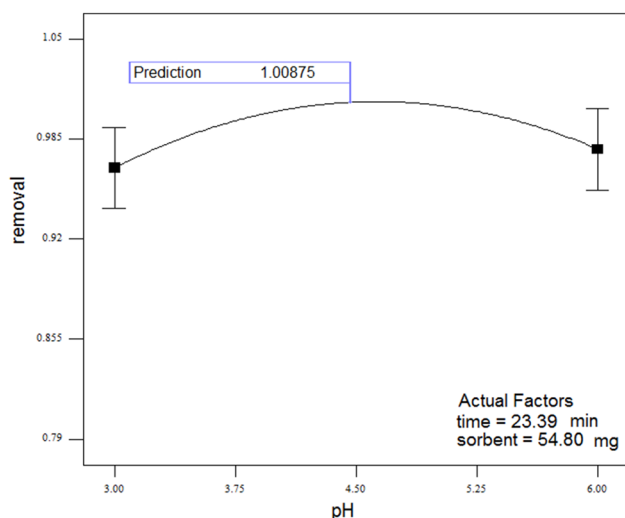


Fig. 7 Effect of pH on removal of Hg(II) ions (aqueous solution volume: 50 mL, stirring rate: 350 rpm, initial concentration 2.5 mg L^{-1} , sorbent dosage: 54.80 mg, time: 23.39 min, temperature: $25 \text{ }^\circ\text{C}$)

Partially lower removal at lower pH values can be attributed to decrease of negative charge density on the adsorbent, as well as the competence of H^+ ions with mercury ions for negatively charged sites on the adsorbent (Hoffmann et al. 2006). Therefore, the optimum pH value was selected as 4.47 for later studies. For this aim the pH was adjusted by HNO_3 (0.01 mol L^{-1}) or NaOH (0.01 mol L^{-1}), 54.80 mg of the dry sorbent was added to 50 ml of solution with 2.5 mg L^{-1} initial concentration of mercury.

Effect of Contact Time

Contact time is another variable which is considered to be highly important in the removal process. The significance of contact time on removal efficiency and yield is already well-known and optimization of this factor will contribute remarkably to the final result. In this work, the effect of contact time was studied in between 10 and 25 min at pH value of 4.47. The removal efficiency of mercury versus contact time presented in Fig. 8 with the initial concentration of 2.5 mg L^{-1} of Hg(II) in 50 mL at $25 \text{ }^\circ\text{C}$ with $\text{pH} = 4.47$. As can be seen the removal of mercury enhanced at a gentle slope upon increasing contact time from 10 to 25 min. At 23.39 min, adsorption value of 99% was already reached, which is why the experiment was not carried on any further. Thus, the optimum contact time was selected as 23.39 min for next studies.

Effect of Sorbent Dose

Other than pH of the solution and contact time of sorbent with the target specie, concentration of the sorbent plays

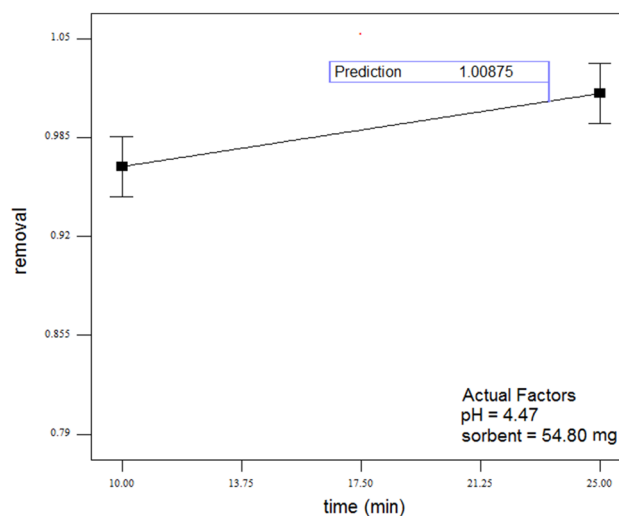


Fig. 8 Effect of contact time on removal of Hg(II) ions (aqueous solution volume: 50 mL, stirring rate: 350 rpm, initial concentration mercury: 2.5 mg L^{-1} , sorbent dosage: 54.80 mg, initial pH: 4.47, temperature: $25 \text{ }^\circ\text{C}$)

an important role in the wastewater treatment and removal process. In this work, we studied the effect of the sorbent dose in between 25 and 55 mg at a 50 mL of solution with an initial concentration of 2.5 mg L^{-1} mercury in ambient temperature ($25 \text{ }^\circ\text{C}$) and previously obtained optimum pH and contact time conditions as 4.47 and 23.39 min, respectively. Figure 9 provides the results for effect of sorbent dose, which indicate the gentle improvement of mercury removal by increasing the dose from 25 mg to 55 mg. Hence, 109.6 mg L^{-1} (54.80 mg) was selected as the optimum dose of the sorbent for removal of mercury.

Three dimensional (3D) and contour plots were drawn to investigate effects of the three parameters on the removal of mercury from water through response surface methodology. Figure 10a shows 3D and (Fig. 10b) contour plots for combined effects of pH values of the solution and contact time on removal of mercury at constant sorbent dose (54.80 mg). One can clearly observe linear increase of the removal as a factor of contact time from 10 min to 25 min. Removal of mercury furthermore enhances by increasing pH values of the solution. At contact time of 23.39 min, the maximum removal occurs at $\text{pH} = 4.47$.

Combined effects of contact time and sorbent dose are demonstrated in Fig. 11 and a constant pH value of 4.47 was selected for this study. Evidently, removal of mercury is a direct factor of both contact time and sorbent dose. The removal improves by increasing the contact time from 10 min to 25 min. On the other hand, increasing sorbent dose from 25 mg to 55 mg enhances the removal linearly.

Figure 12 illustrates combined effects of pH values of the solution and sorbent dose on the removal of mercury at

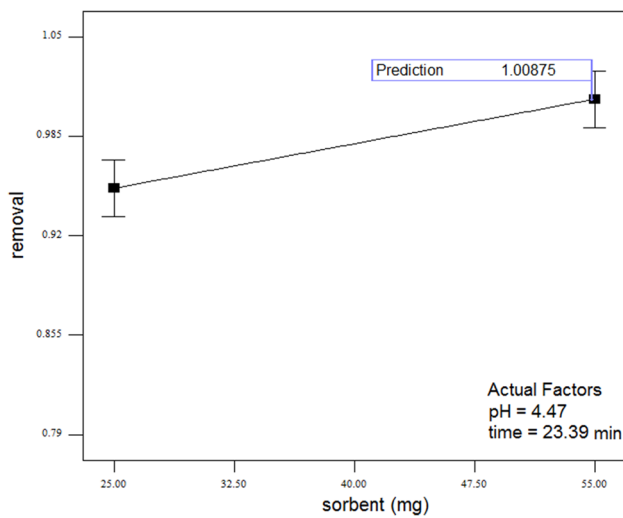


Fig. 9 Effect of adsorbent dose on removal of Hg(II) ions (aqueous solution volume: 50 mL, stirring rate: 350 rpm, initial concentration mercury: 2.5 mg L⁻¹, initial pH: 4.47, time: 23.39, temperature: 25 (°C))

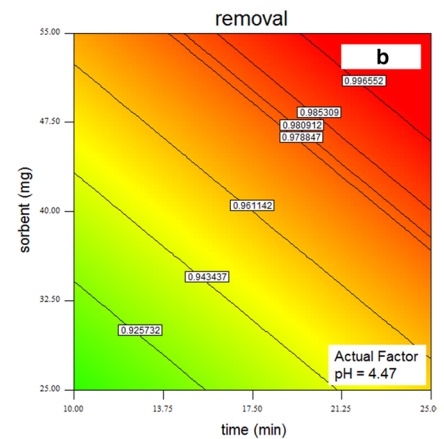
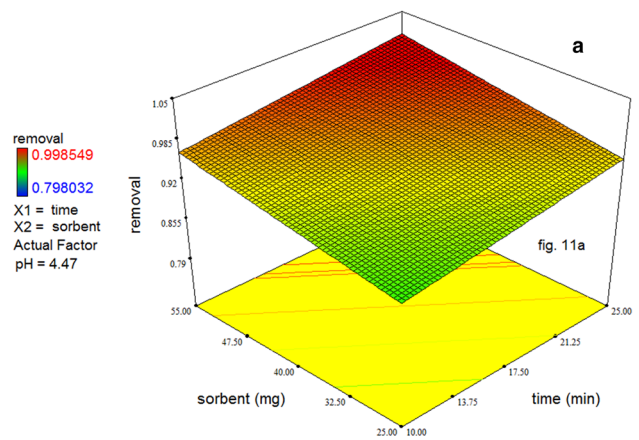


Fig. 11 a 3D and b contour plots of combined effects of adsorbent dose and contact time on removal of Hg(II) ions

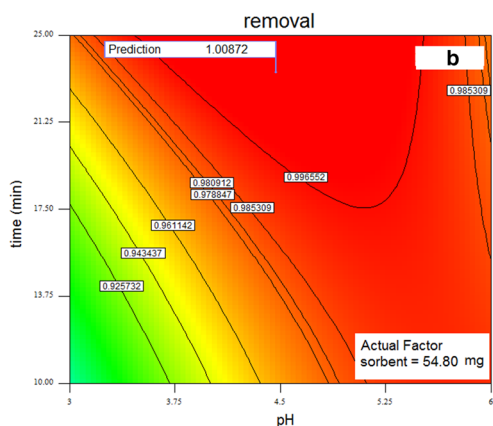
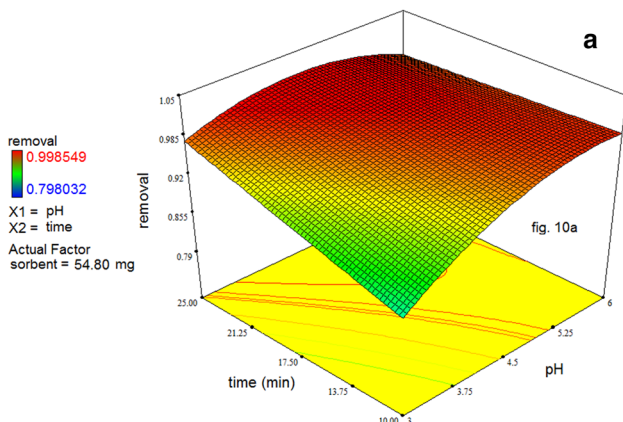


Fig. 10 a 3D and b contour plots of combined effects of pH value of the solution and contact time on removal of Hg(II) ions

a constant contact time of 23.39 min. As observed before, removal of mercury increases as a direct function of the sorberent dose and reaches the maximum value at sorberent dose of 55 mg. On the other hand, the removal increased upon increasing the pH values from 3 to 4.5, where the maximum removal took place. Following further increase of the pH value, removal of mercury declined. Thus, it is evident from the plots that maximum mercury removal was obtained at sorberent dose of 55 mg and pH value of 4.47.

The primary objective of this work was obtained from the optimum condition of three independent variables for removal of mercury from water. Table 6 presents range and level of the parameters under study to reach the optimum condition.

Langmuir and Freundlich Isotherm Models

It is possible to successfully apply Langmuir isotherm model to equilibrium adsorption by assuming monolayer adsorption on identical sites on the sorberent. The equation is given as follows:

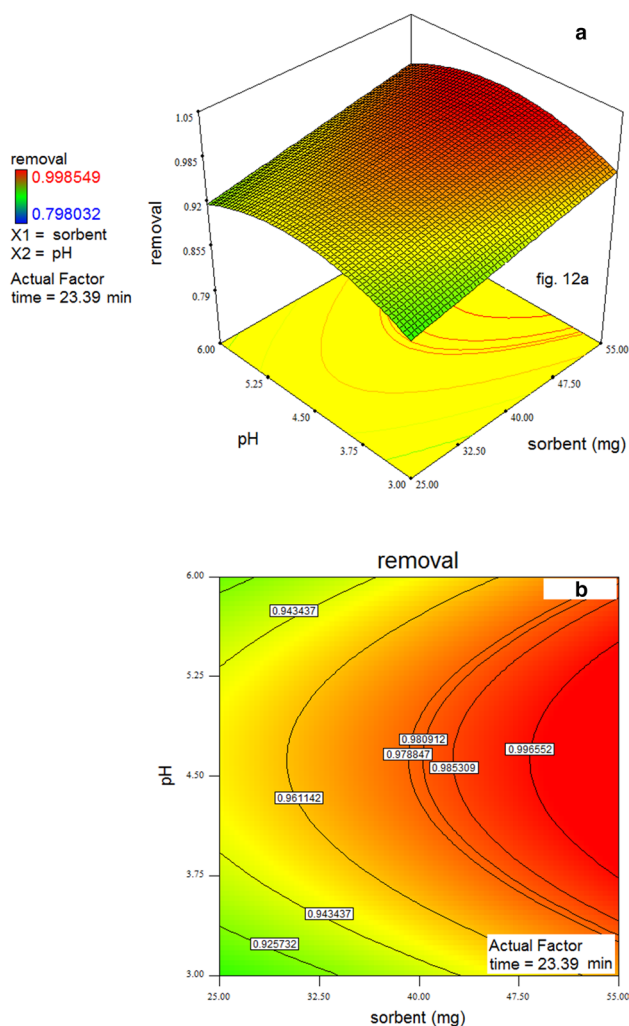


Fig. 12 a 3D and b contour plots of combined effects of adsorbent dose and pH value of the solution on removal of Hg(II) ions

$$\frac{C_e}{q_e} = \frac{1}{q_m K_L} + \frac{C_e}{q_m}, \tag{6}$$

where C_e stands for equilibrium concentration of Hg(II) ions solution (mg L^{-1}), and q_m is the maximum value for Hg(II) adsorption on a certain amount of sorbent (mg g^{-1}). q_e is the

equilibrium adsorption amount at heavy metal equilibrium concentration (mg g^{-1}) and K_L is the Langmuir adsorption constant (L mg^{-1}). The values of q_m and K_L were calculated from the slope and intercept of the Langmuir plot of C_e versus C_e/q_e (Esmaeili et al. 2017).

Equilibrium parameter (R_L) is the essential characteristic of the Langmuir isotherm that can be shown in terms of a dimensionless constant named separation factor, and is calculated as;

$$R_L = \frac{1}{1 + K_L C_0}, \tag{7}$$

where C_0 is the initial concentration of ions (mg L^{-1}). The values of R_L shows the shape of adsorption isotherms to be either irreversible ($R_L = 0$), favorable ($0 < R_L < 1$), linear ($R_L = 1$) or unfavorable ($R_L > 1$). According to the obtained results, the calculated values of R_L were found to be between 0 and 1 (Vojoudi et al. 2017).

On the other hand, the Freundlich model is an empirical equation for the description of equilibrium on heterogeneous surfaces. The logarithmic form of Freundlich equation is as follows:

$$\log(q_e) = \log(K_f) + \frac{1}{n} \log C_e, \tag{8}$$

where $\frac{1}{n}$ and K_f are the slopes of intercept of the plot, respectively (Bhatti et al. 2017).

The results obtained for mercury ion adsorption in current work, according to Table 7 are in relatively more agreement with the Langmuir isotherm model. In the Langmuir model, R^2 was obtained as 0.99 and equilibrium parameter (R_L) was found to lie in between 0 and 1, which further verified the reliability of the model for adsorption of mercury ion from water. According to Langmuir model, maximum adsorption of Hg(II) was obtained as 113.64 mg g^{-1} .

Adsorption Kinetics

In adsorption process, studying adsorption kinetics is important to understand molecular diffusion and chemical reactions taking place in the medium. Kinetic equations further help to

Table 6 The optimum condition

Factor	Name	Level	Low level	High level	Std. Dev.	Coding	
A	pH	4.731930155	3	6	0	Actual	
B	Time	24.67613073	10	25	0	Actual	
C	Sorbent	49.95474204	25	55	0	Actual	
Response	Prediction	SE mean	95% CI low	95% CI high	SE Pred	95% PI low	95% PI high
Removal	1.002735256	0.011231722	0.977327335	1.028143176	0.023297288	0.950033129	1.055437382

Table 7 Isoterm data for removal of Hg(II)

Langmuir constant		Freundlich constant				
R_L (L mg ⁻¹)	q_m (mg g ⁻¹)	R_L	R^2	K_f	n	R^2
0.69	113.64	0.37	0.99	34.05	2.66	0.97

Table 8 Kinetic data for removal of Hg(II)

Pseudo-first order			Pseudo-second order		
k_1	R^2	q_e (mg g ⁻¹)	k_2	R^2	q_e (mg g ⁻¹)
0.172	0.999	1.756	0.384	0.998	25.062

understand effects of different parameters on the reaction rate. In the current work, pseudo-first and second-order equations were used (Eq. 8 and 9, respectively) (Ashraf et al. 2018). Kinetic experiments were performed using 2.5 ppm solutions of Hg(II) ion stirred at 300 rpm for different time ranges under the optimal condition obtained before (Table 8).

$$\ln \frac{q_e - q_t}{q_e} = -k_1 t, \quad (9)$$

where q_e is the adsorption capacity (mg g⁻¹) at equilibrium and q_t is adsorption capacity (mg g⁻¹) at time t , k_1 stands for the rate constant of the equilibrium (min⁻¹) (Hartmann 2005). One can obtain k_1 by simply plotting $\log(q_e - q_t)$ against t .

$$\frac{t}{q_t} = \frac{1}{k_2 q_e^2} + \frac{t}{q_e} \quad (10)$$

where k_2 is the second-order rate constant (Karimi et al. 2015).

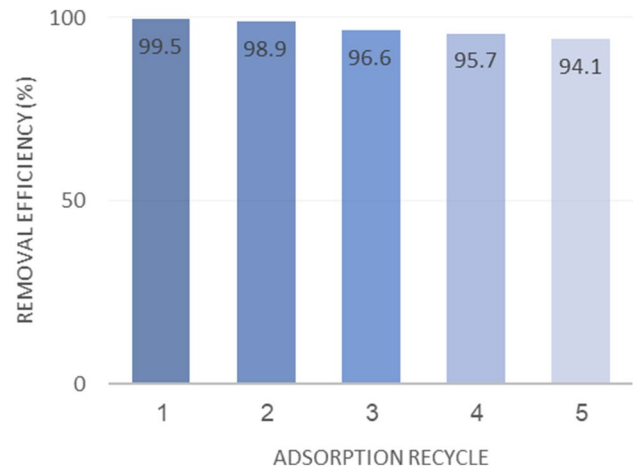
It is possible to evaluate the agreement between experimental and predicted results through R^2 , the equation of which is provided below (Eq. 10);

$$R^2 = \frac{\sum (q_e - q_{tma})^2}{\sum (q_e - q_{tma})^2 + \sum (q_e - q_t)^2}, \quad (11)$$

where q_{tma} is the mean value for q_t .

Selectivity Studies

Adsorption of mercury by the sorbent was studied in the presence of various commonly interfering agents including alkali and alkaline earth metals (Na⁺, K⁺, and Mg(II)), heavy metallic-ions (Pb(II), Cd(II), and Ni(II)), and anions (Cl⁻ and SO₄²⁻) to evaluate selectivity of the sorbent for mercury. For all selectivity studies, 2.5 ppm of Hg(II) ion and 1 M solutions of the nitrate salt of cations, as well as sodium salts of anions were used. All experiments were performed at the optimum removal conditions obtained

**Fig. 13** Reusing the modified LUS-1 after acid washing

before. The results obtained, revealed that the tested potential interfering agents barely influenced adsorption of mercury by the sorbent except for Cl⁻ anion. This may be attributed to the strong tendency of chloride ion to interact with mercury ions and form HgCl₂ and/or Hg₂Cl₂, impeding Hg(II) ions from being adsorbed on the surface of the sorbent, which in turn results in lower adsorption.

Reusability

Reusability is another highly important factor for an adsorbent to be practically applied in water treatment, which can reduce costs, remarkably. Hence, recovery of the current sorbent and its reusability was investigated. Nitric and chloric acids were used in pretests to select the most appropriate acid to remove the adsorbed Hg(II) ion from the sorbent. After filtration of the sorbent particles from the suspension, the filter paper was placed in acetone and sonicated to remove all particles from the filter. The acetone was then evaporated off on a heater to obtain the dry powder. The obtained powder was treated with acid, washed with deionized water, and finally dried at 60 °C. The test was carried out for five repeats and metal recovery of the sorbent was calculated after each recovery via the following equation:

$$R = \frac{A}{B} \times 100, \quad (12)$$

Table 9 Analysis of effluent of bandar Emam petrochemical unite

Sample	pH	Temperature (°C)	Cations and anions (ppm)							
			Hg(II)	Cd(II)	Cr(II)	Na(II)	Ni(II)	Pb(II)	Cl ⁻ (g L ⁻¹)	SO ₄ ²⁻ (g L ⁻¹)
Untreated	6.5	31	16.5	< 0.01	< 0.01	41730	< 0.02	< 0.05	93.4	6.6
Treated	1	33	1.2	0.01	0.01	75400	0.02	0.126	51.3	7.5

Table 10 Removal of Hg(II) ion from real samples

Sample	Initial concentration (ppm)	Remaining concentration (ppm)	Removal efficiency (%)
Untreated	16.5	7.051	57.26
Treated	1.2	0.08	93.30

where A is the amount of the removed metal-ion from the sorbent, and B is the amount of the adsorbed metallic-ion.

Figure 13 shows the modified adsorbent can be reused more than 5 times without considerable reduction in removal efficiency.

Real Sample Studies

The efficiency of the sorbent in the removal of mercury was furthermore investigated in the real sample medium. The real sample water used in this work was provided by Bandar Emam Petrochemical Unite and used for the tests without any dilution. The compositions of real sample are presented in Table 9. The test was carried out under optimum conditions obtained through RSM studies. pH of the sample was adjusted by 0.1 M solutions of NaOH and nitric acid. As observed in Table 10 this sorbent is capable of functioning in real environments and remove mercury ion from real media efficiently.

Conclusion

In the current work, a novel sorbent was developed by incorporation of sulfur-containing groups into the pore channels of LUS-1, which is a meso-porous silica material with high specific surface area. The successful synthesis of the sorbent was verified by several characterization analyses such as BET, low-angle powder XRD, SEM, FT-IR, and TGA. Effects of three independent variables (pH of the solution, contact time, and sorbent dose) on removal of Hg(II) ion from water were investigated through RSM. The results obtained from RSM studies confirmed the appropriateness of the model. The optimum condition for the removal of Hg(II) ion was obtained as pH = 4.47, 23.39 min contact time, and 54.80 mg sorbents. Adsorption isotherms were

studied and the maximum Hg(II) adsorption was calculated as 113.64 mg g⁻¹ based on Langmuir isotherm model. Pseudo-first and second-order equations were used to investigate the adsorption kinetics. Furthermore, results of reusability and real sample test indicated high efficiency and promising potential of the sorbent for real environment applications.

Acknowledgements The authors acknowledge scientific and financial support provided by the University of Tehran and Parseen (Pars Environment, Energy and Nanotechnology) Corporation.

References

- Abry S, Albela B, Bonneviot L (2005) Toward dual function patterning onto surface of as-made mesostructured silica. *C R Chim* 8(3–4):741–752. <https://doi.org/10.1016/j.crci.2004.12.008>
- Antochshuk V, Olkhovik O, Jaroniec M, Park I-S, Ryoo R (2003) Benzoylthiourea-modified mesoporous silica for mercury(II) removal. *Langmuir* 19(7):3031–3034
- Badiei A, Bonneviot L, Crowther N, Ziarani GM (2006) Surface tailoring control in micelle templated silica. *J Organomet Chem* 691(26):5911–5919
- Badiei A, Gholami J, Khaniani Y (2009) Synthesis and characterization of titanium supported on high order nanoporous silica and application for direct oxidation of benzene to phenol. *E-J Chem* 6(s1):S324–S328. <https://doi.org/10.1155/2009/292483>
- Baei MS, Esfandian H, Nesheli AA (2016) Removal of nitrate from aqueous solutions in batch systems using activated perlite: an application of response surface methodology. *Asia-Pac J Chem Eng* 11(3):437–447
- Bhatti IA, Ahmad N, Iqbal N, Zahid M, Iqbal M (2017) Chromium adsorption using waste tire and conditions optimization by response surface methodology. *J Environ Chem Eng* 5(3):2740–2751. <https://doi.org/10.1016/j.jece.2017.04.051>
- Bidhendi ME, Bidhendi GRN, Mehrdadi N, Rashedi H (2014) Modified *Mesoporous Silica* (SBA-15) with Trithiane as a new effective adsorbent for mercury ions removal from aqueous environment. *J Environ Health Sci Eng* 12(1):100
- Carvalho CM, Chew EH, Hashemy SI, Lu J, Holmgren A (2008) Inhibition of the human thioredoxin system a molecular mechanism of mercury toxicity. *J Biol Chem* 283(283):11913–11923
- Clarkson TW, Magos L, Myers GJ (2003) The toxicology of mercury—current exposures and clinical manifestations. *N Engl J Med* 349(18):1731–1737
- Di Natale F, Lancia A, Molino A, Di Natale M, Karatza D, Musmarra (2006) Capture of mercury ions by natural and industrial materials. *J Hazard Mater* 132(2–3):220–225
- Ding J, Li H, Wang C, Yang J, Xie Y, Peng Q, Li Q, Li Z (2015) “Turn-On” fluorescent probe for mercury(II): high selectivity and sensitivity and new design approach by the adjustment of the π -bridge. *ACS Appl Mater Interfaces* 7(21):11369–11376

- Driscoll CT, Mason RP, Chan HM, Jacob DJ, Pirrone N (2013) Mercury as a global pollutant: sources, pathways, and effects. *Environ Sci Technol* 47:4967–4983
- Esmaeeli F, Gorbanian SA, Moazezi N (2017) Removal of estradiol valerate and progesterone using powdered and granular activated carbon from aqueous solutions. *Int J Environ Res*. <https://doi.org/10.1007/s41742-017-0060-0>
- Fu F, Wang Q (2011) Removal of heavy metal ions from wastewaters: a review. *J Environ Manag* 92(3):407–418
- Gholami J, Badieli A, Abbasi A, Ziarani GM (2009) Synthesis and characterization of VOx/LUS-1 nanoporous silica and application for direct oxidation of benzene to phenol. *Int J Chem Tech Res* 1(3):426–429
- Hamad B, Alshebani A, Pera-Titus M, Wang S, Torres M, Albela B, Bonneviot L, Miachon S, Dalmon JA (2008) Synthesis and characterization of nanocomposite MCM-41 ('LUS') ceramic membranes. *Microporous Mesoporous Mater* 115(1–2):40–50. <https://doi.org/10.1016/j.micromeso.2007.11.047>
- Hartmann M (2005) Ordered mesoporous materials for bioadsorption and biocatalysis. *Chem Mater* 17(18):4577–4593
- Hoffmann F, Cornelius M, Morell J, Fröba M (2006) Silica-based mesoporous organic–inorganic hybrid materials. *Angew Chem Int Ed* 45(20):3216–3251
- Hosseini M, Ganjali MR, Rafiei-sarmazdeh Z (2013) A novel Lu 3 + fluorescent nano-chemosensor using new functionalized mesoporous structures. *Anal Chim Acta* 771:95–101. <https://doi.org/10.1016/j.aca.2013.01.064>
- Huang Y, Du JR, Zhang Y, Lawless D, Feng X (2015) Removal of mercury (II) from wastewater by polyvinylamine-enhanced ultrafiltration. *Sep Purif Technol* 154:1–10
- Kadirvelu K, Thamaraiselvi K, Namasivayam C (2001) Removal of heavy metals from industrial wastewaters by adsorption onto activated carbon prepared from an agricultural solid waste. *Biores Technol* 76(1):63–65
- Karimi M, Badieli A, Lashgari N, Afshani J, Ziarani GM (2015) A nanostructured LUS-1 based organic–inorganic hybrid optical sensor for highly selective sensing of Fe³⁺ in water. *J Lumin* 168:1–6
- Morris RE, Wheatley PS (2008) Gas storage in nanoporous materials. *Angew Chem Int Ed* 47(27):4966–4981
- Nakanishi K, Tanaka N (2007) Sol–gel with phase separation. Hierarchically porous materials optimized for high-performance liquid chromatography separations. *Account Chem Res* 40(9):863–873
- Parlett CM, Wilson K, Lee AF (2013) Hierarchical porous materials: catalytic applications. *Chem Soc Rev* 42(9):3876–3893
- Raji F, Pakizeh M (2013) Study of Hg(II) species removal from aqueous solution using hybrid ZnCl₂-MCM-41 adsorbent. *Appl Surf Sci* 282:415–424
- Sabri MA, Ibrahim TH, Khamis MI, Al-Asheh S, Hassan MF (2018) Use of *Eucalyptus Camaldulensis* as biosorbent for lead removal from aqueous solution. *Int J Environ Res*. <https://doi.org/10.1007/s41742-018-0112-0>
- Sahu J, Acharya J, Meikap B (2009) Response surface modeling and optimization of chromium (VI) removal from aqueous solution using Tamarind wood activated carbon in batch process. *J Hazard Mater* 172(2–3):818–825
- Saleh TA, Sari A, Tuzen M (2017) Optimization of parameters with experimental design for the adsorption of mercury using polyethylenimine modified-activated carbon. *J Environ Chem Eng* 5(1):1079–1088
- Shahabuddin S, Tashakori C, Kamboh A, Sotoudehnia Z, Saidur R, Nodeh HR, Bidhendi ME (2018) Kinetic and equilibrium adsorption of lead from water using magnetic metformin-substituted SBA-15. *Environ Sci Water Res Technol* 4:549–558
- Shiravand G, Badieli A, Ziarani GM, Jafarabadi M, Hamzehloo M (2012) Photocatalytic synthesis of phenol by direct hydroxylation of benzene by a modified nanoporous silica (LUS-1) under sunlight. *Chin J Catal* 33(7–8):1347–1353. [https://doi.org/10.1016/S1872-2067\(11\)60422-1](https://doi.org/10.1016/S1872-2067(11)60422-1)
- Vojoudi H, Badieli A, Bahar S, Ziarani GM, Faridbod F, Ganjali MR (2017) A new nano-sorbent for fast and efficient removal of heavy metals from aqueous solutions based on modification of magnetic *Mesoporous silica* nanospheres. *J Magn Magn Mater* 441:193–203. <https://doi.org/10.1016/j.jmmm.2017.05.065>
- Zhang Q, Wu J, Luo X (2016) Facile preparation of a novel Hg(II)-ion-imprinted polymer based on magnetic hybrids for rapid and highly selective removal of Hg(II) from aqueous solutions. *RSC Adv* 6:14916–14926